LIGHT FRONT VARIABLES IN HIGH ENERGY HADRoN-HADRON AND NUCLEUS-NUCLEUS INTERACTIONS

L.Chkhaidze[1], T.Djobava[1], V.Garsevanishvili [2], L.Kharkhelauri[1] Yu.Tevzadze[1]

[1] *High Energy Physics Institute, Tbilisi State University,*
University Str. 9, 380086 Tbilisi, Georgia
[2] *Mathematical Institute of the Georgian Academy of Sciences*
M.Alexidze Str. 1 , 380093 Tbilisi, Georgia

E-mail: Tamar.Djobava@cern.ch

ABSTRACT

Light front variables are introduced to study inclusive spectra of secondaries in hadron-hadron and nucleus-nucleus interactions. It is established that the phase space of secondary pions is divided into two parts with significantly different characteristics. The thermal equilibrium seems to be reached in one of these parts. Corresponding temperatures of pions in hadron-hadron and nucleus-nucleus collisions are extracted. The results are compared with the results of other types of analysis. The results for nucleus-nucleus collisions are compared with the predictions of the Quark-Gluon String Model (QGSM). The QGSM satisfactorily reproduces the experimental data for light and intermediate-mass nuclei.

1.INTRODUCTION. DEFINITION AND PROPERTIES OF VARIABLES.

An important role in establishing of many properties of multiple production is played by the choice of kinematic variables in terms of which observable quantities are presented (see e.g. [1,2]). The variables which are commonly used are the following: the Feynman $x_F = 2p_z/\sqrt{s}$, rapidity $y = \frac{1}{2}\ln[(E+p_z)/(E-p_z)]$, transverse scaling variable $x_T = 2p_T/\sqrt{s}$ etc. In the case of azimuthal symmetry the surfaces of const x_F are the planes $p_z = x_F\sqrt{s}/2$, surfaces of constant y are the hyperboloids

$$p_z^2\left[\left(\frac{1+e^{2y}}{1-e^{2y}}\right)^2 - 1\right] - p_T^2 = m^2$$

and the surfaces of constant x_T are the planes $p_T = x_T\sqrt{s}/2$ in the phase space.

At high energies different dynamical mechanisms contribute to spectra of secondaries. Among them "pionization" and fragmentation mechanisms are widly discussed. "Pionization" means the existence of secondary pions with relatively low momenta and flat (almost isotropic) angular distribution in the centre of mass frame of colliding objects. The fragmentation component has sharply anisotropic angular distribution in the centre of mass frame. One of the principal problems in this direction is the separation of these two components. Up to now there exits no unique way to separate these mechanisms. Different authors propose different ways and non of them seems to be satisfactory. It will be shown that the presentation of inclusive spectra in terms of light front variables provides an unique possibility to separate these two components.

Unified scale invariant variables for the presentation of single particle inclusive distributions have been proposed [3], the properties of which are described below.

Consider an arbitrary 4–momentum $p_\mu(p_0, \vec{p})$ and introduce light front combinations [4]:

$$p_\pm = p_0 \pm p_3 \tag{1}$$

If the 4–momentum p_μ is on the mass shell ($p^2 = m^2$), the combinations $p_\pm$, $\vec{p}_T$ (where $\vec{p}_T = (p_1,\ p_2)$) define the so called horospherical coordinate system (see, e.g. [5,6]) on the corresponding mass shell hyperboloid $p_0^2 - \vec{p}^{\,2} = m^2$ ($u = \frac{p}{m}$, $u_0^2 - \vec{u}^{\,2} = 1$). Corresponding hyperboloid in the velocity space is the realization of the curved space with constant negative curvature, i.e. the Lobachevsky space.

Let us construct scale invariant variables:

$$\xi^{\pm} = \pm \frac{p^c_{\pm}}{p^a_{\pm} + p^b_{\pm}} \tag{2}$$

in terms of the 4–momenta $p^a_\mu,\ p^b_\mu,\ p^c_\mu$ of particles $a,\ b,\ c$, entering the inclusive reaction $a + b \to c + X$. The z-axis is taken to be the collision axis, i.e. $p_z = p_3$. Particles a and b can be hadrons, heavy ions, leptons.

It is interesting to note the properties of $\xi^{\pm}$ - variables in some limiting cases. The light front variables $\xi^{\pm}$ in the centre of mass frame are defined as follows [3]:

$$\xi^{\pm} \ = \ \pm \frac{E \pm p_z}{\sqrt{s}} = \pm \frac{E + |p_z|}{\sqrt{s}} \tag{3}$$

where s is the usual Mandelstam variable, $E = \sqrt{p_z^2 + p_T^2 + m^2}$ and p_z are the energy and the z - component of the momentum of produced particle. The upper sign in Eq. (3) is used for the right hand side hemisphere and the lower sign for the left hand side hemisphere.

In order to enlarge the scale in the region of small $\xi^{\pm}$, it is convenient also to introduce the variables

$$\zeta^{\pm} = \mp \ln |\xi^{\pm}| \tag{4}$$

The invariant differential cross section in terms of these variables looks as follows:

$$E \frac{d\sigma}{d\vec{p}} = \frac{|\xi^{\pm}|}{\pi} \ \frac{d\sigma}{d\xi^{\pm} dp_T^2} = \frac{1}{\pi} \ \frac{d\sigma}{d\zeta^{\pm} dp_T^2} \tag{5}$$

In the limits of high p_z ($|p_z| \gg p_T$) and high p_T ($p_T \gg |p_z|$) the $\xi^{\pm}$ variables go over to the well known variables,

$$\xi^{\pm} \to \tfrac{2p_z}{\sqrt{s}} = x_F \ ; \ \xi^{\pm} \to \tfrac{m_T}{\sqrt{s}} \to \tfrac{p_T}{\sqrt{s}} = \tfrac{x_T}{2} \ ; \ m_T = \sqrt{p_T^2 + m^2}$$

respectively, which are intensively used in high energy physics. $\xi^{\pm}$–variables are related to x_F, x_T and rapidity y as follows:

$$\xi^{\pm} \ = \ \frac{1}{2} \left(x_F \pm \sqrt{x_F^2 + x_T^2} \right) \ ; \ x_T = \frac{2m_T}{\sqrt{s}} \tag{6}$$

$$y \ = \ \pm \frac{1}{2} \ln \frac{(\xi^{\pm} \sqrt{s})^2}{m_T^2} \tag{7}$$

The region $|\xi^{\pm}| < m/\sqrt{s}$ is kinematically forbidden for the $\xi^{\pm}$–spectra integrated over all values of p_T^2, and the region $|\xi^{\pm}| < m_T/\sqrt{s}$ is forbidden for the $\xi^{\pm}$–spectra at fixed values of p_T^2. The minimum value of $\xi^{\pm} = \pm \frac{m}{\sqrt{s}}$ we call the threshold value.

Light front variables have been introduced by Dirac [4] and they are widely used now in theoretical studies of relativistic composite systems (see, e.g.[7-11], in theoretical and experimental studies of nuclear reactions with beams of relativistic nuclei.

Inclusive structure functions of γ-quanta, $\pi^{\pm}$, K^0 mesons and Λ-hyperons in $\pi^- - p$ interactions at 5 and 40 GeV/c [12] and of $\pi^{\pm}$ mesons in pp collisions at 22.4 GeV/c [13] has been analysed in terms of light front variables.

2. ANALYSIS OF PION DISTRIBUTIONS IN TERMS OF LIGHT-FRONT VARIABLES

The study of π^- mesons produced in the relativistic nucleus-nucleus collisions in terms of the light front variables [14,15]has been performed. The choice of the light front variables is due to the fact, that as one can see from the prevoius section, these variables seem to be more sensitive to the dynamics of interaction as compared to the well-known Feynman variable x_F and rapidity y. The analysis has been carried out in the nucleus-nucleus centre of mass system for π^- mesons from He(Li,C), C-Ne, Mg-Mg, C-Cu and O-Pb collisions [14] obtained on the SKM-200-GIBS facility of JINR and for π^- mesons from p-C, He-C, C-C and C-Ta collisions collected with the two metre Propane Bubble Chamber (PPK-500) of JINR [15].

SKM-GIBS consists of a 2 m streamer chamber, placed in a magnetic field of 0.8 Tesla, and a triggering system [14].

In Fig. 1 the $\xi^{\pm}$ – distribution of π^- mesons from Mg-Mg interactions is presented. These distributions are similar for all analysed pairs of nuclei. One can see from Fig. 1, that the principal differences of $\xi^{\pm}$ distributions as compared to the corresponding x_F – distributions are the following:

(1) existence of some forbidden region around the point $\xi^{\pm} = 0$;

(2) existence of maxima at some $\tilde{\xi^{\pm}}$ in the region of relatively small $|\xi^{\pm}|$.

3) existence of limits for $|\xi^{\pm}| \leq m/\sqrt{s})$, similarly to hadron-hadron collisions.

The experimental data for invariant distribution $(1/\pi)\cdot dN/d\zeta^{\pm}$ is shown in Fig. 2. The curve is the result of the polynomial approximation of the experimental distributions. The maxima at $\tilde{\zeta}^{\pm}$ are also observed in the invariant distributions $(1/\pi)\cdot dN/d\zeta^{\pm}$. However, the region $|\xi^{\pm}| > |\tilde{\xi}^{\pm}|$ goes over to the region $|\zeta^{\pm}| < |\tilde{\zeta}^{\pm}|$ and vice versa (see Eqs. (3) and (4)). The value of maxima are observed at $\tilde{\zeta^{\pm}} = 2.0 \pm 0.1$ for all pairs of nuclei. The $\tilde{\zeta^{\pm}}$ is the function of the energy (see Eqs. (3), (4)) and does not depend on the mass numbers of the projectile (A_P) and target (A_T).

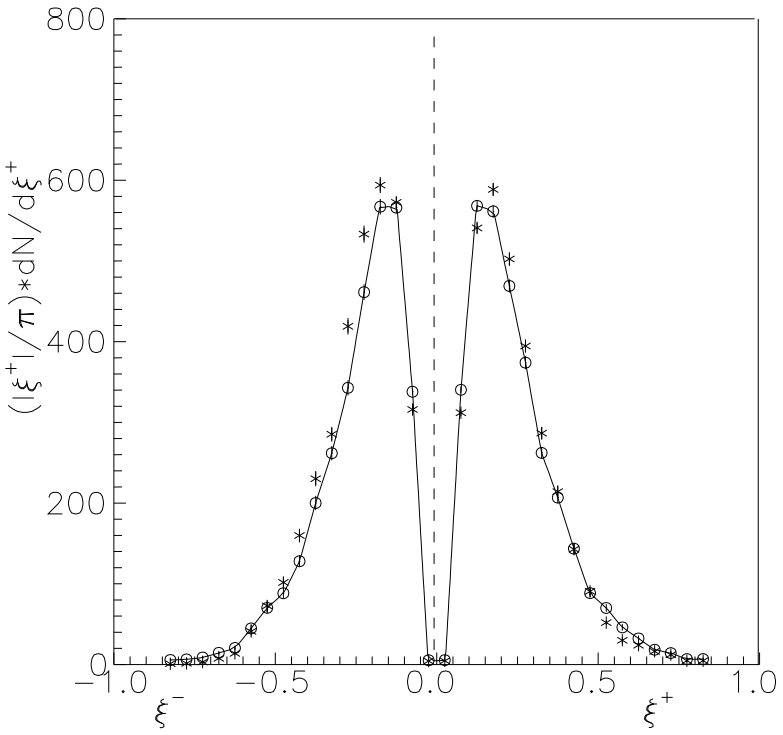

Figure 1: The $\xi^{\pm}$ – distribution of π^- mesons from Mg-Mg interactions. $\circ$ – experimental data, $\star$ – QGSM data. The curve is a result of polinomial approximation of the experimental data.

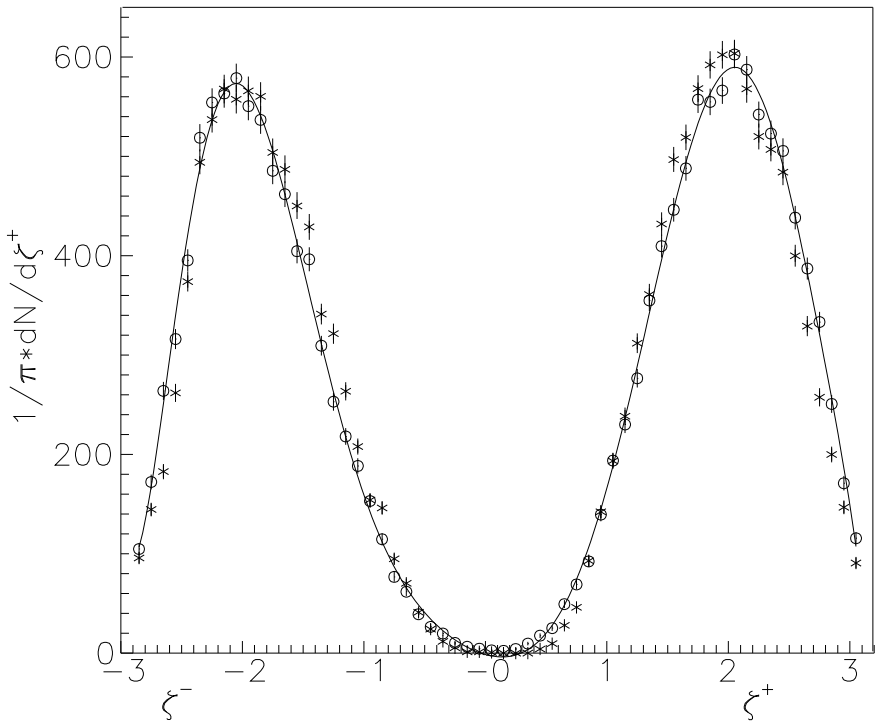

Figure 2: The $\zeta^{\pm}$ distribution of π^- mesons from Mg-Mg interactions. $\circ$ – experimental data, $\star$ – QGSM data. The curve – result of polinomial approximation of the experimental data.

In order to study the nature of these maxima the phase space has been divided into two parts $|\zeta^{\pm}| > |\tilde{\zeta^{\pm}}|$ ($\tilde{\zeta^{+}}$= 2.0) and $|\zeta^{\pm}| < |\tilde{\zeta^{\pm}}|$ and the p_T^2 and the angular distributions of π^- mesons in these regions have been studied separetely. The number of pions in these two regions are approximately equal. For example in C-Cu interactions in the region $|\zeta^{\pm}| > |\tilde{\zeta^{\pm}}|$ the number of pions is equal to –1987 and in $|\zeta^{\pm}| < |\tilde{\zeta^{\pm}}|$ — 2212. In Figs. 3 and 4 the p_T^2 and the angular distributions of π^- mesons from Mg-Mg, interactions in different regions of ζ^+ ($\zeta^+ > \tilde{\zeta^+}$ and $\zeta^+ < \tilde{\zeta^+}$) in the forward hemisphere are presented.

One can see from Figs. 3 and 4, that the p_T^2 and the angular distributions of π^- mesons differ significantly in $\zeta^+ > \tilde{\zeta^+}$ and $\zeta^+ < \tilde{\zeta^+}$ regions. The angular distribution of pions in the region $\zeta^+ < \tilde{\zeta^+}$ (Fig.4) is sharply anisotropic in contrast to the almost flat distribution in the region $\zeta^+ > \tilde{\zeta^+}$ (Fig. 4). The flat behaviour of the angular distribution allows one to think that one observes a partial thermal equilibrium in the region $|\zeta^{\pm}| > |\tilde{\zeta^{\pm}}|$ ($|\xi^{\pm}| < |\tilde{\xi^{\pm}}|$) of phase space. The slopes of p_T^2 – distributions differ greatly in different regions of $\zeta^{\pm}$ (Fig. 3). For example in Mg-Mg interactions: $< p_T^2 >= (0.027 \pm 0.002)$ (GeV/c)^2 in the region $\zeta^+ > \tilde{\zeta^+}$; $< p_T^2 >= (0.103 \pm 0.009)$ (GeV/c)^2 in the region $\zeta^+ < \tilde{\zeta^+}$.

Note, that the surfaces of constant $\xi^{\pm}$ are the paraboloids

$$p_z^c = \frac{p_\perp^{c^2} + m^{c^2} - (\xi^{\pm}\sqrt{s})^2}{-2\xi^{\pm}\sqrt{s}} \tag{8}$$

in the phase space. Thus the paraboloids:

$$p_z^c = \frac{p_\perp^{c^2} + m^{c^2} - (\tilde{\xi^+}\sqrt{s})^2}{-2\tilde{\xi^+}\sqrt{s}} \tag{9}$$

separates two groups of particles with significantly different characteristics. Thus in the $\zeta^{\pm}$ ($\xi^{\pm}$) distributions we have singled out points $\tilde{\zeta^{\pm}}$ ($\tilde{\xi^{\pm}}$) which seperate in the phase space two groups of particles with significantly different features. There are no such points in the x_F and y -distributions.

To describe the spectra in the region $\xi^+ < \tilde{\xi^+}(\zeta^+ > \tilde{\zeta^+})$ the simplest statistical model with the Boltzman $f(E) \sim e^{-E/T}$ and the Bose-Einstein $f(E) \sim (e^{E/T} - 1)^{-1}$ distributions has been used.

The distributions $\frac{1}{\pi}\frac{d\sigma}{d\zeta^+}$, $\frac{d\sigma}{dp_T^2}$ and $\frac{d\sigma}{d\cos\Theta}$ look in this region as follows :

$$\frac{1}{\pi}\frac{d\sigma}{d\zeta^+} \sim \int_0^{p_{T,max}^2} Ef(E)dp_T^2, \tag{10}$$

$$\frac{d\sigma}{dp_T^2} \sim \int_0^{p_{z,max}} f(E)dp_z, \tag{11}$$

$$\frac{d\sigma}{d\cos\Theta} \sim \int_0^{p_{max}} f(E)p^2dp, \tag{12}$$

$$E = \sqrt{\vec{p}^2 + m_\pi^2}\ ,\ \vec{p}^2 = p_z^2 + p_T^2 \tag{13}$$

where:

$$p^2_{T,max} = (\xi^+\sqrt{s})^2 - m^2_\pi \tag{14}$$

$$p_{z,max} = \frac{p^2_T + m^2_\pi - (\tilde{\xi}^+\sqrt{s})^2}{-2\tilde{\xi}^+\sqrt{s}} \tag{15}$$

$$p_{max} = \frac{-\tilde{\xi}^+\sqrt{s}\cos\Theta + \sqrt{(\tilde{\xi}^+\sqrt{s})^2 - m^2_\pi \sin^2\Theta}}{\sin^2\Theta} \tag{16}$$

The experimental distributions $\frac{1}{\pi}\frac{d\sigma}{d\zeta^+}$, $\frac{d\sigma}{dp^2_T}$ and $\frac{d\sigma}{d\cos\Theta}$ in the region $\xi^+ < \tilde{\xi}^+(\zeta^+ > \tilde{\zeta}^+)$ have been fitted by Eqs. (10), (11) and (12), respectively. The results of the fit given in Table 1 and Figs. 3,4,5 show satisfactory agreement with experiment. Thus the spectra of $\pi^\pm$–mesons in the region $\xi^+ < \tilde{\xi}^+(\zeta^+ > \tilde{\zeta}^+)$ are satisfactorily described by the formulae which follow from the statistical model. The same formulae when extrapolated to the region $\xi^+ > \tilde{\xi}^+(\zeta^+ < \tilde{\zeta}^+)$ deviate from the data.

The similar analysis of π^- meson spectra produced in p-C, He-C, C-C and C-Ta interactions at a momentum of 4.2 GeV/c/nucleon has been carried out in light-front variables [15]. The data have been obtained using the 2-metre Propane Bubble Chamber of JINR (Dubna), placed in a magnetic field of 1.5 Tesla. The chamber, which housed tantalum targets of thickness about 1mm, was irradiated with protons, deuterons and by relativistic He and C nuclei of incident momenta that varied between 2 and 10 GeV/c per nucleon. From the whole ensemble of collisions of C nuclei in Propane Chamber an inelastic C-C collisions have been selected. The pionts have been singled out $\tilde{\zeta^\pm}$: $\tilde{\zeta^\pm}$=2.0 for p-C, $\tilde{\zeta^\pm}$=1.8 – He-C, $\tilde{\zeta^\pm}$=1.9 – C-C and $\tilde{\zeta^\pm}$=2.0 – C-Ta. The spectra of pions have been described with the same formulae, as for SKM-200-GIBS data, and the parameters T $(\zeta^+ > \tilde{\zeta^+})$ and n $(\zeta^+ < \tilde{\zeta^+})$ have been extraced. The results of fits are presented in Table 1. One can see (Table 1), that the results of SKM-200-GIBS and of 2-m Propane Bubble Chamber Collaboration (PPK-500) agree quite well. The angular and transverse momentum distributions of π^- mesons in various regions of variables $\xi^\pm$ and $\zeta^\pm$ in p-C, He-C, C-C and C-Ta collisions show the characterists (behaviour) [15] similar to those from He(Li,C), C-Ne, Mg-Mg, C-Cu and O-Pb collisions of SKM-200-GIBS experiment.

The Quark Gluon String Model [16] was used for the comparison with experiemntal data of SKM-200-GIBS. He(Li,C), C-Ne, Mg-Mg, C-Cu and O-Pb interactions have been generated using Monte-Carlo generator COLLI, based on the QGSM. The QGSM reproduces the p^2_T and $cos\Theta$ distributions (Figs.3 anf 4) and shows the similar characteristics in the different regions of ζ as experimental ones.

One can see from the Table 1, that the values of the T extracted from the experimental and QGSM data coincide within the errors.

In Fig. 6 the dependence of the parameter T from the Tables 5 and 6 on $(A_P * A_T)^{1/2}$, obtained from the experimental and QGSM data of SKM-200-GIBS and experimental results of PPK-500, is presented. One can see, that T decreases linearly with the increasing $(A_P * A_T)^{1/2}$ i.e with the increasing number of participating nucleons. Similar behaviour is predicted by the QGSM.

Table 1. Number of the events, trigger and the results of the joint fit of the distributions $1/\pi \cdot dN/d\zeta^+$, dN/dp_T^2, $dN/dcos\Theta$ of π^- – mesons by Eq. (10), (11), (12) in the region $\zeta^+ > \tilde{\zeta^+}$.

$A_p - A_T$ $T(\Theta_{ch}, \Theta_n)$		Number of events	T (MeV) $\zeta^+ > \tilde{\zeta^+}$
$p - C(propane)$	exp.	8371	89 ± 20
$He(Li, C)$	exp.	6147	81 ± 2
$T(2, 0)$	QGSM	15566	84 ± 2
$He - C(propane)$	exp.	13318	87 ± 3
$C - C(propane)$	exp.	20594	72 ± 2
$C - Ne$	exp.	902	79 ± 3
$T(2, 0)$	QGSM	3950	82 ± 2
$Mg - Mg$	exp.	6261	76 ± 2
$T(2, 2)$	QGSM	6212	77 ± 2
$C - Cu$	exp.	1203	72 ± 2
$T(3, 3)$	QGSM	3463	74 ± 2
$C - Ta(propane)$	exp.	1989	64 ± 4
$O - Pb$	exp.	732	55 ± 3

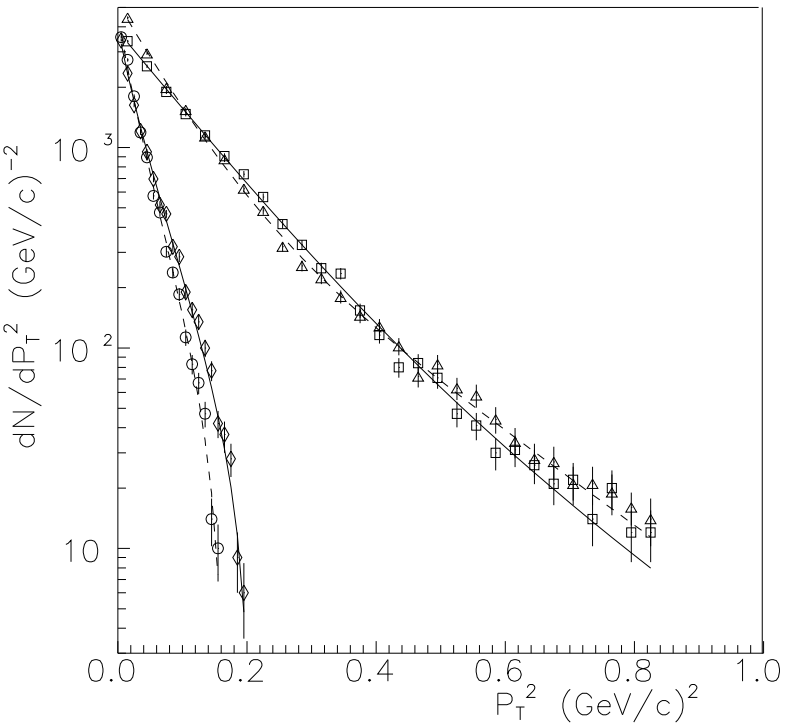

Figure 3: The p_T^2 distribution of π^- mesons from Mg-Mg interactions. $\circ$ – experimental data for $\zeta^+ > \tilde{\zeta^+}$ ($\tilde{\zeta^+}$=2.0); $\diamond$ – the QGSM data for $\zeta^+ > \tilde{\zeta^+}$; $\triangle$ – experimental data for $\zeta^+ < \tilde{\zeta^+}$; $\square$ – the QGSM data for $\zeta^+ < \tilde{\zeta^+}$. Dashed lines: fit of the experimental data by the Boltzmann distribution. Solid lines: fit of the QGSM data by the Boltzmann distribution.

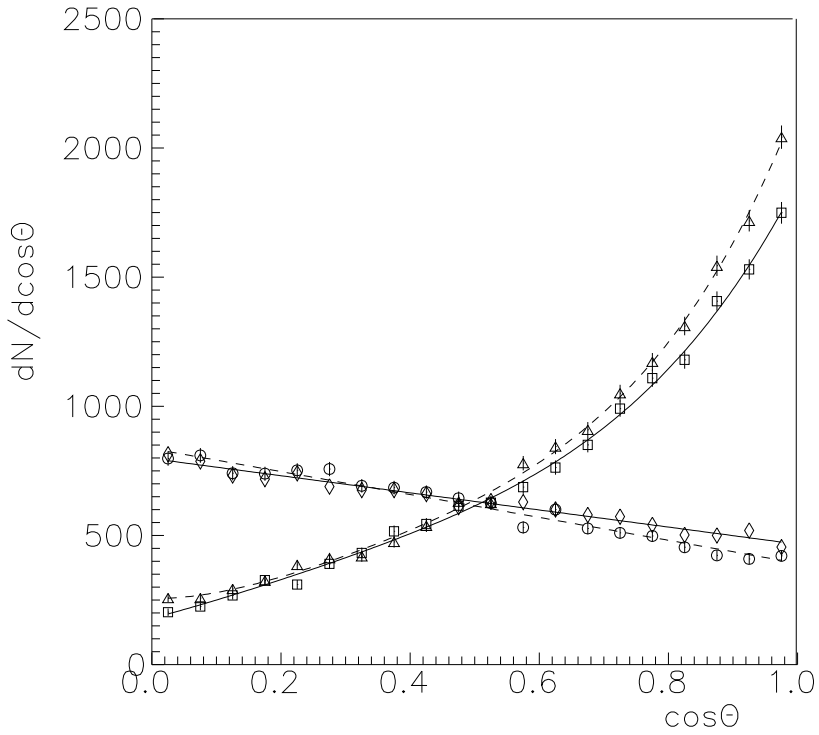

Figure 4: The $cos\Theta$ distribution of π^- mesons from Mg-Mg interactions. $\circ$ – experimental data for $\zeta^+ > \tilde{\zeta^+}$ ($\tilde{\zeta^+}$=2.0); $\diamond$ – the QGSM data for $\zeta^+ > \tilde{\zeta^+}$; $\triangle$ – experimental data for $\zeta^+ < \tilde{\zeta^+}$; $\square$ – the QGSM data for $\zeta^+ < \tilde{\zeta^+}$. Dashed lines:fit of the experimental data by the Boltzmann distribution. Solid lines:fit of the QGSM data by the Boltzmann distribution.

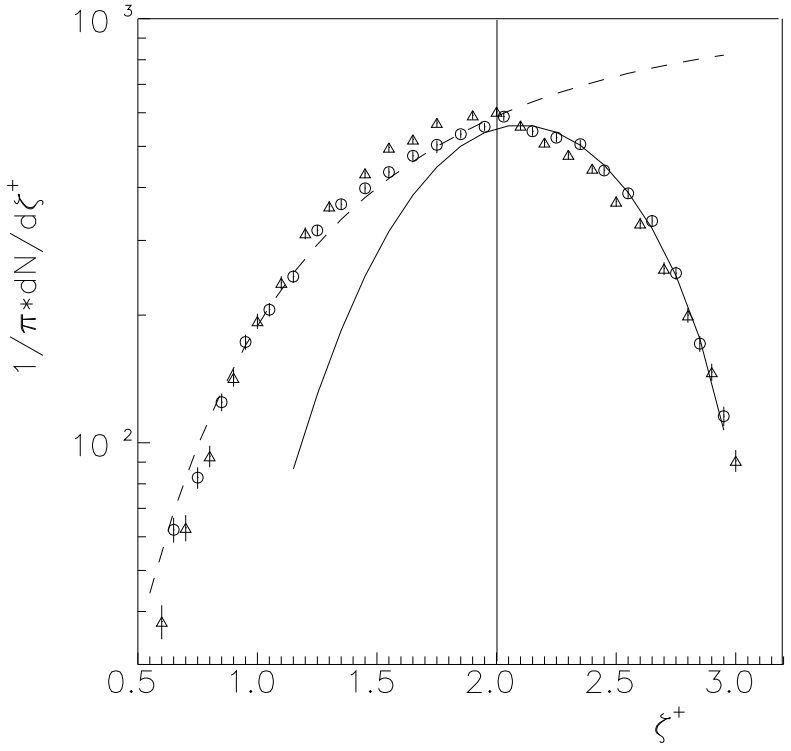

Figure 5: The $(1/\pi) \cdot dN/d\zeta^+$ distribution of π^- mesons from Mg-Mg interacti
experimental data; solid line – fit of the data in the region $\zeta^+ > \tilde{\zeta^+}$ by the E
distribution; the dashed line – fit of the data in the region $\zeta^+ < \tilde{\zeta^+}$ by the
$(1 - e^{-|\zeta^+|})^n$; $\triangle$ – QGSM data.

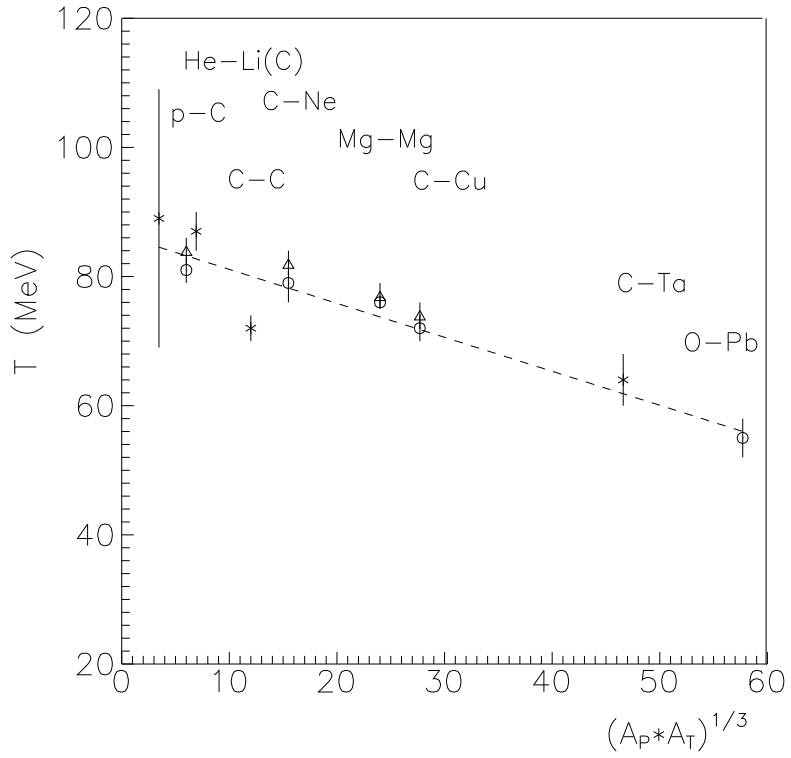

Figure 6: The dependence of the parameter T on $(A_P * A_T)^{1/2}$ for He(Li,C), C-
Mg, C-Cu and O-Pb [14]: $\circ$ – the experimental data, $\triangle$ – the QGSM data;
He-C, C-C and C-Ta [15]: $*$ – the experimental data. The dashed line is a result
approximation.

3. CONCLUSION

A remark on the nature of maxima in $\zeta^{\pm}$ -distributions is in order. The ALEPH Collaboration observed the maxima in the ξ - distributions ($\xi = -ln\ p/p_{max}$) [17] of secondary hadrons in $e^+\ e^-$ collisions, which coincide to high precision with predictions of the perturbative QCD. The accuracy of coincidence increases when next to leading order corrections are taken into account. So the shapes of ξ - distributions are related to the details of the underlying dynamics. Similarly, it seems that the maxima in $\zeta^{\pm}$ -distributions reflect the dynamics of the processes considered. In particular, secondary pions with $|\xi^{\pm}| < |\tilde{\xi}^{\pm}|$ have almost flat angular distribution in the centre of mass frame, whereas pions with $|\xi^{\pm}| > |\tilde{\xi}^{\pm}|$ are produced sharply anisotropically. So the phase space of secondary pions is divided into two parts with significantly different characteristics in an unique way. Separation points are points of maxima in corresponding $\xi^{\pm}(\zeta^{\pm})$-spectra (or corresponding paraboloids in the phase space). Thus one can say that the problem of separation of "pionization" and fragmentation components seems to be solved in an unique way. An application of the method proposed to a wide class of hadronic and nucleus-nucleus reactions and e^+e^--annihilation into hadrons seems to be of great interest.

In conclusion, we think that the use of light front variables can help to distinguish in between different dynamical contributions, or test basic principles in other types of analysis, such as two-particle correlations, HBT-interferometry [18,19] and transverse flow studies [20]. It seems to be interesting to perform the above analysis for future experiments ATLAS and ALICE at CERN LHC.

References

[1] A.M. Baldin, Nucl. Phys. A447 (1985) 203

[2] A.A. Baldin, Phys. of Atomic Nuclei, 56 (1993) 385

[3] L.N.Abesalashvili, N.S.Amaglobeli, L.T.Akhobadze, V.R.Garsevanishvili et al.,In: Proc. of IV European Antiproton Symposium, Strasburg, 1978

[4] P.A.M. Dirac, Rev. Mod. Phys. 21 (1949) 392

[5] N. Ya. Vilenkin and Ya. A. Smorodinsky, Sov. J. of Exp. and Theor. Physics, JETP 46 (1964) 1793

[6] V.R. Garsevanishvili, V.G. Kadyshevsky, R.M. Mir-Kasimov and N.B. Skachkov, Sov. J. of Theor. and Math. Phys. 7 (1971) 203

[7] H. Leutwyler, Nucl. Phys. B76 (1974) 413

[8] V.R. Garsevanishvili, A.N. Kvinikhidze, V.A. Matveev, A.N. Tavkhelidze and R.N. Faustov, Sov. J. of Theor. and Math. Phys. 23 (1975) 310

[9] V.R. Garsevanishvili and V.A. Matveev, Sov. J. of Theor. and Math. Phys. 24 (1975) 3

[10] V.R. Garsevanishvili and Z.R. Menteshashvili, Relativistic Nuclear Physics in the Light Front Formalism, (Nova Science Publishers, New York, 1993)

[11] J. Carbonell, B. Desplanques, V.A. Karmanov and J.-F. Mathiot, Phys. Rep. 300 (1998) 215; nucl-th/9804029

[12] L. Abesalashvili, N. Amaglobeli, V. Garsevanishvili et al., JETP Letters v.30 (1979) 448;
L. Abesalashvili, N. Amaglobeli, V. Garsevanishvili et al., Sov. J. Nucl.Phys. v.30 (1979) 156

[13] N. Amaglobeli, Sh. Esakia, V. Garsevanishvili et al., Eur.Phys.J., 1999, v.8C, p.603-607

[14] M.Anikina, L.Chkhaidze, T. Djobava, V.Garsevanishvili et al., Nucl.Phys. A640 (1998) 117;
M.Anikina, L.Chkhaidze, T. Djobava, V.Garsevanishvili et al., Eur.Phys.J. A7 (2000) 139

[15] L.Akhobadze, V.Garsevanishvili,... Yu.Tevzadze et al., Phys. of Atomic Nuclei 63(2000)1670

[16] Amelin N. et al., Sov.J. Nucl.Phys. v.52 (1990) 272

[17] Z. Ajaltouni et al.,ALEPH Collaboration. CERN/PPE 96-186; Phys.Rep. 294 (1998) 1

[18] R.Hanbury-Brown and R.Twiss, Phil.Mag. 45 (1954) 663

[19] G.I.Kopylov and M.I.Podgoretsky, Sov.J. Nucl.Phys. 19 (1974) 215

[20] P.Danielewicz and G.Odyniec, Phys. Lett. B157 (1985) 146